Resonant charge transfer in He^+-He collisions studied with the merging-beams technique

R. D. Rundel, D. E. Nitz,* K. A. Smith, M. W. Geis,† and R. F. Stebbings
Space Physics and Astronomy Department, Rice University, Houston, Texas 77001
(Received 17 April 1978)

Absolute cross sections are reported for the resonant charge-transfer reaction $He^+ + He \rightarrow He + He^+$ at collision energies between 0.1 and 187 eV. The results, obtained using a new merging-beam apparatus at Rice University, are in agreement both with theory and with measurements made using other experimental techniques. The experimentally determined cross sections between 0.5 and 187 eV fall about a line given by $\sigma^{1/2}(\text{Å}^2) = 5.09 - 2.99 \ln W$, where W is the collision energy in eV. Considerable attention is paid to the configuration and operation of the apparatus. Tests and calculations which confirm the interpretation of the experimental data in a merging-beam experiment are discussed.

I. INTRODUCTION

Resonant charge-transfer processes represent perhaps the simplest form of chemical reaction and have been the subjects of intensive theoretical and experimental studies. Experimental investigation of these processes at low collision energies remains a formidable task; consequently, there exist very few charge-transfer cross-section measurements in the collision energy range between room temperature and a few eV. The merging-beam technique is particularly well suited to the study of atomic collisions in this energy range. In this paper, we describe a new merging-beam apparatus and report measured absolute cross sections for the reaction

$$He^+ + He \rightarrow He + He^+ \quad (1)$$

at collision energies between 0.1 and 200 eV.

The concept of studying collision processes at low relative velocities by observing the interaction between two collinear beams of particles traveling in the same direction was first employed in an abortive study of electron-ion recombination in 1929,[1] but largely forgotten until 1959 when Cook and Ablow[2] suggested that it could be advantageously applied to the study of heavy-particle collisions. The application of the merging-beam technique to investigation of collisions in the energy range between 0.01 and 100 eV has been discussed extensively in the literature[3] and here we shall give only a brief outline of the technique.

The technique requires production of two superimposed beams of particles, each having relatively high (~1–10 keV) energy in the laboratory frame of reference, arranged such that the beams have nearly identical velocities. The collision energy W of the reacting species in the center of mass reference frame is given by

$$W = \tfrac{1}{2}\mu v_r^2 , \quad (2)$$

where μ is the reduced mass of the collision partners and v_r is their relative velocity. In terms of particle energies in the laboratory frame

$$W = \frac{m_1 m_2}{m_1 + m_2}\left[\left(\frac{E_1}{m_1}\right)^{1/2} - \left(\frac{E_2}{m_2}\right)^{1/2}\right]^2 , \quad (3)$$

where m_i and E_i are, respectively, the mass and energy of the particles in beam i. If we define a normalized laboratory frame energy difference

$$\Delta E = (m_2/m_1)E_1 - E_2 , \quad (4)$$

then if $\Delta E/E_2 \ll 1$, the collision energy is given to a good approximation by

$$W \approx \frac{1}{4E_2}\left(\frac{m_1}{m_1 + m_2}\right)\Delta E^2 . \quad (5)$$

The transformation of the laboratory-frame energies to the center-of-mass reference frame produces a so-called energy deamplification—that is, the center-of-mass collision energy is smaller than ΔE by a factor on the order of $4E_2/\Delta E$.

An analogous deamplification effect reduces the uncertainty in W caused by the fact that the primary beams are not monoenergetic but contain particles having kinetic energies within narrow ranges $E_1 \pm \delta E_1$ and $E_2 \pm \delta E_2$. The energy widths of the primary beams introduce an uncertainty in ΔE given by

$$\delta(\Delta E) = (m_2/m_1)\delta E_1 + \delta E_2 . \quad (6)$$

The corresponding uncertainty δW in the interaction energy is approximately

$$\delta W \approx (\mu \Delta E/2E_1 m_1)\delta(\Delta E) . \quad (7)$$

Thus the energy spreads of the primary beams are reduced by a factor on the order of $\Delta E/E$ when the collision is viewed in the center-of-mass frame.

In a merging-beam experiment, the uncertainty in the collision energy arises not only from the

beam energy spreads but also from the fact that the colliding beams each possess some angular divergence and collisions may occur between particles traveling on paths which cross at some angle θ. Such collisions have a slightly different interaction energy than those which take place between particles on truly collinear trajectories, and this difference in interaction energy is given by

$$\Delta W(\theta) = \frac{m_1 m_2}{m_1 + m_2}\left(\frac{E_1 E_2}{m_1 m_2}\right)^{1/2}\theta^2 . \tag{8}$$

A precise evaluation of the mean uncertainty in W for a particular experiment is a rather difficult task. For the present experiment, however, one can easily show that the maximum possible value of $\Delta W(\theta)$ represents a small fraction of the collision energy W. Numerical examples of the relations between the laboratory beam energies E_1 and E_2, their energy spreads δE_1 and δE_2, the corresponding center-of-mass collision energies W, and the net uncertainty in W are given in Table I for operating conditions used in the present experiment.

In a merging-beam experiment the collision cross section σ and the experimentally determined parameters are related by the expression

$$\sigma = (S/F)v_1 v_2/|v_1 - v_2| , \tag{9}$$

where S is the measured product formation rate, v_1 and v_2 are the beam velocities, and F is a quantity known as the overlap integral, defined by

$$F = \int J_1(x,y,z)J_2(x,y,z)\,dx\,dy\,dz , \tag{10}$$

where J_1 and J_2 are the reactant beam fluxes in particles/cm^2 sec and the integration is carried out over the volume in which the measured product is formed.

TABLE I. Considerations determining collision energy in the present experiment. E_1 and E_2 are the ion and neutral beam energies, respectively, W is the collision energy, and δW and $\Delta W(\theta)$ are the uncertainties in W associated with the beam energy spreads and beam divergences, respectively. The ion and neutral beam energy spreads are taken to be 2 eV. All values given are in eV.

E_1	E_2	W	δW	$\Delta W(\theta)$ $\theta = 0.003$
1265	3014	186.9	1.38	0.009
940	1509	33.5	0.61	0.005
2445	3014	14.9	0.23	0.012
1220	1509	7.7	0.24	0.006
1336	1509	2.6	0.09	0.006
1402	1509	1.0	0.08	0.007
1434	1509	0.5	0.05	0.007
1476	1509	0.09	0.02	0.007

II. APPARATUS

Figure 1 is a schematic diagram of the apparatus configured for study of the $He^+ + He \rightarrow He + He^+$ reaction. The neutral beam originates as an ion beam extracted from a medium-pressure ($\sim 5\times 10^{-2}$ Torr) magnetically confined arc ion source. This source produces a relatively intense (~ 1-μA) ion beam with a narrow (~2-eV) energy spread, and can produce beams of a wide variety of atomic and molecular ions. Ions emerging from the source are accelerated and focused by a set of 2.2-in.-diam electrostatic cylindrical lenses which render the beam parallel as it enters the first bending magnet.

The beam is then momentum analyzed by a pair of 60° sector magnets. Use of two magnets instead of the conventional single magnet has several advantages in a merging-beam experiment. The optical arrangement of the magnet pair is that of a telescope of unit magnification; that is, the downstream focal point of the first magnet coincides with the upstream focal point of the second. Therefore a parallel beam of the proper momentum entering the magnet system is essentially unaltered by passage through the magnets, but particles having undesired momenta are deflected out of the beam. The magnet pair has a momentum resolution $\Delta P/P$ of about 10^{-2}. Careful scanning of the profiles of beams passed by the magnet pair indicates that, for beams of the intended momentum the magnets do not focus the beam, and that the beam geometry is controlled primarily by the electrostatic lenses near the ion source. The absence of magnetic focusing is of course particularly important in a merging-beam experiment since, for good collision energy resolution, beams of minimal divergence are required.

The fast neutral beam is produced by charge transfer of the momentum-analyzed ion beam in a gas cell, which is maintained at a pressure such that a substantial fraction (5%–20%) of the ions passing through the cell are converted to fast neutrals. The ions remaining in the beam are electrostatically removed at the cell exit. Although this manner of neutral-beam production has several drawbacks it remains the most practical method currently available. The primary difficulty lies in the fact that the relative population of ground- and excited-state neutrals is generally unknown. Therefore, in using neutral beams produced by charge transfer, one must carefully examine the possibility that observed reaction signals may reflect contributions from many states of the neu-

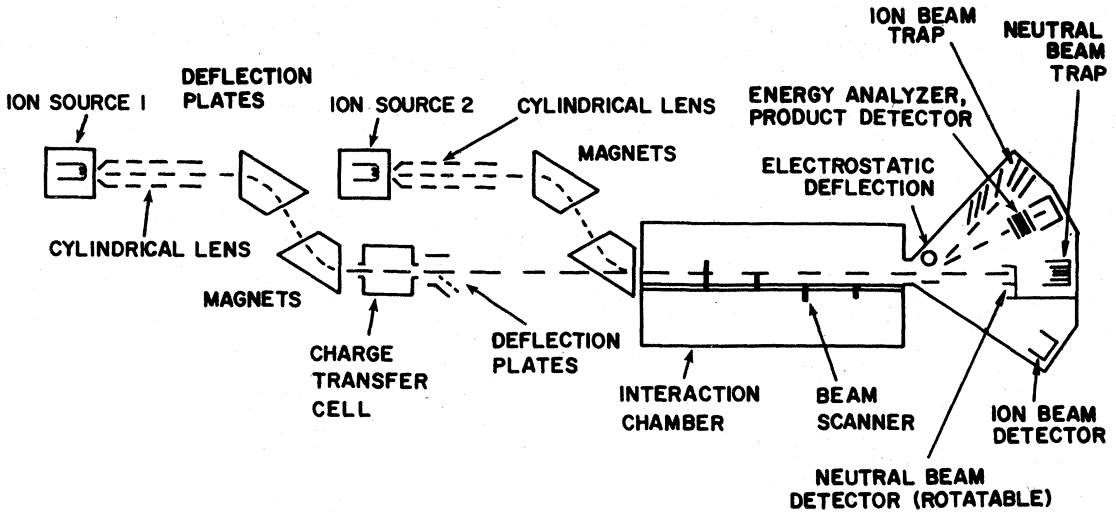

FIG. 1. Schematic diagram of merging-beam apparatus.

tral reactant.

As discussed subsequently, the importance of excited neutral species has been assessed, and it is concluded that for the present experiment, excited-state reactants do not significantly affect the cross section determination.

After its generation, the neutral beam is collimated by two 5-mm-diam apertures separated by a distance of 60 cm, so that the maximum possible neutral beam divergence is about 0.01 rad. Observed divergences are typically 0.003 rad.

The reactant ion beam is produced in an electron-impact ion source very similar to the source developed by Carlston and Magnuson.[4] The lens and magnet arrangements for the ion beam are essentially identical to those used in the other beam line. The ion and neutral beams are merged in the second momentum analysis magnet, and travel together throughout a 1-m-long interaction chamber.

It is important that the background gas pressure in this chamber be as low as possible, since collisions between the background gas and the parent beams may cause unwanted background. In order to minimize the pressure in the interaction region, two stages of differential pumping are interposed between the ion-beam source and the interaction region, and there are four stages of differential pumping between the charge-transfer cell and the interaction region. The interaction region and detection chambers employ double o-ring seals and are routinely baked for 3–10 H at ~100 °C. The detection and interaction chambers are pumped by LN_2-trapped 6-in.(NRC VHS-6) diffusion pumps. Typical operating pressure in these chambers is 2×10^{-9} Torr.

At the end of the interaction region the ion and neutral beams are separated in an electrostatic field. The field used in the present experiment is produced between a positively biased plate and a negatively biased cylinder. The product beam is directed through a five-grid retarding potential analyzer and onto a Johnston Laboratories MM-1 electron multiplier. The multiplier output pulses are then amplied and counted. The primary function of the energy analyzer is rejection of backgrounds due to stripping of the neutral beam by the background gas in the interaction region. Even though the pressure of background gas in the interaction region is low, about 1 part in 10^7 of the parent He beam is converted to He^+ in the process

$$He + X \rightarrow He^+ + X + e^- - 24.5\ \text{eV}, \qquad (11)$$

where X represents the residual gas. The amount of He^+ formed in the stripping reaction (11) is three to five orders of magnitude larger than the amount formed in the charge-transfer process under study, and some means for discriminating against the stripped He^+ must be provided in order to perform an experiment in a reasonable length of time. The energetics of process (11) dictate that the He^+ formed must lose an amount of translational energy greater than the ionization potential of the incident neutral He. For example if the He beam energy is 3000 eV, the He^+ resulting from (11) will have a lab-frame translational energy

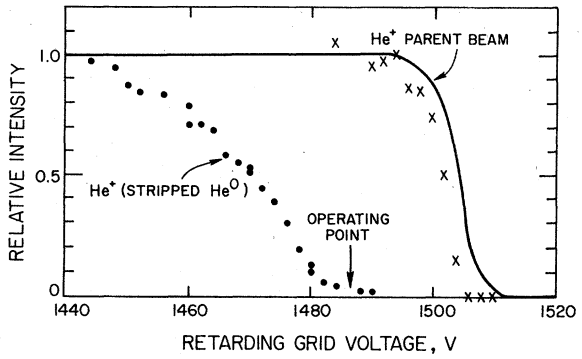

FIG. 2. Energy-analyzer transmission for various beam components. He^+ beam, 1500 eV energy; • , stripped He^0 beam, X, signal from reaction (1).

of less than 2976 eV. Figure 2 shows a typical energy-analyzer output for the stripping background and for the signal resulting from process (1). Clearly the analyzer can be set to reject the majority of the He^+ produced by stripping while accepting almost all of the signal.

The energy analyzer also serves to reject signal arising from collisions involving excited neutral helium. This discrimination occurs because the excited-state neutrals are formed (in the He-filled gas cell) in an endothermic process.

$$He^+ + He \rightarrow He^* + He - \sim 20 - 25 \text{ eV} \qquad (12)$$

and, by the same argument as that applicable to stripped ions, must have lab-frame translational energies at least 20–25 eV less than those ground-state neutrals formed in resonant collisions. Thus the charged product of a reaction involving one of these excited neutrals such as

$$He^+ + He^* \rightarrow He^* + He^+ \qquad (13)$$

would also possess a lower lab energy than the product of reaction (1) and would therefore be rejected by the energy analyzer.

III. MEASURED QUANTITIES

As shown in Eq. (9), a cross-section determination at a given collision energy requires measurement of the overlap integral, the beam velocities and the signal production rate.

The method used to determine the overlap integral has been described in detail elsewhere.[5] The apparatus is shown in Fig. 3. Mounted on a motor-driven shaft in the interaction chamber are four pie-shaped stainless-steel plates, each having nine small (~1-mm-diam) apertures evenly spaced at increasing radial distances from the center of the shaft. As the shaft turns, each hole moves along a different path through the superimposed beams. The sampled currents from each beam (the neutral beam flux is monitored by secondary electron ejection) are fed to an analog multiplier whose output is proportional to the integrand of Eq. (10). Each scanner plate thus samples the two-dimensional beam overlap at a different position in the interaction region. The three-dimensional overlap integral F is then determined by integrating the set of two-dimensional overlaps over the entire interaction length. An example is shown in Fig. 4. An evaluation of F requires only about

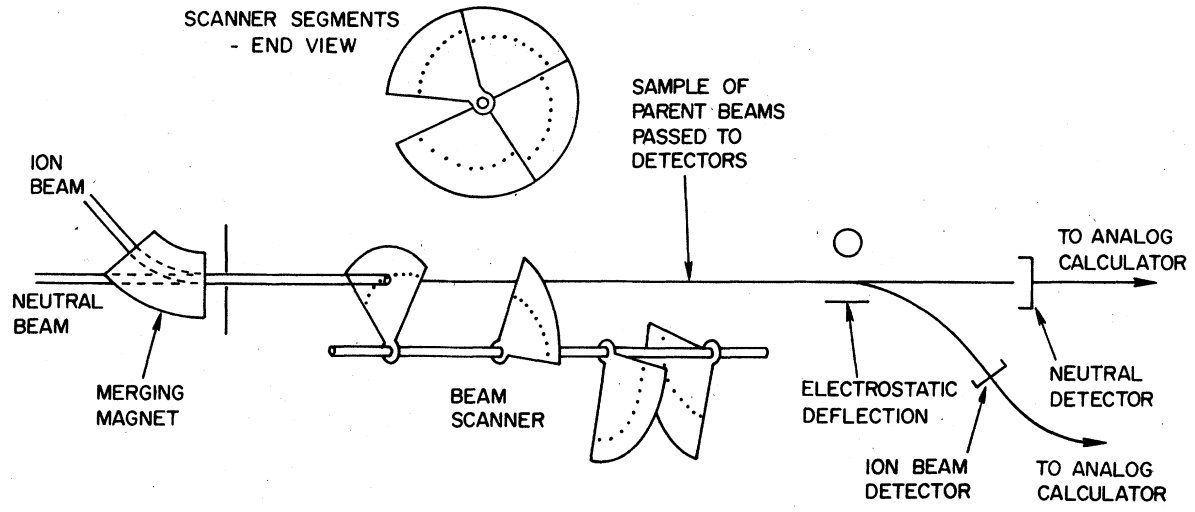

FIG. 3. Overlap integral measuring apparatus.

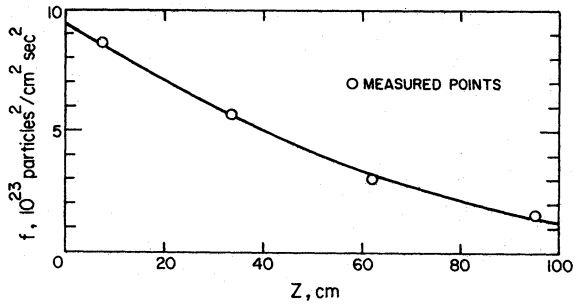

FIG. 4. Measured two-dimensional overlap integral as a function of interaction region length. Solid curve is a fit to data points. The three-dimensional overlap integral corresponds to the area under the curve.

5 min and it is repeated periodically throughout the process of data accumulation. The values of F thus determined are found to depend strongly on beam alignment. Since the beam alignment may vary slightly in the course of several hours of data accumulation, the facility for frequent measurement of F is crucial to the process of accurate cross-section measurement.

The beam velocities are usually calculated from the ion-source operating potentials, but they are periodically determined by direct measurement of beam energy with the retarding potential analyzer. This measurement also yields estimates of the ion-source plasma potentials and the energy spreads in the beams emerging from the ion sources. Typically the ion-source plasma potentials do not differ significantly from that of the source body, and measured beam energy spreads are $\lesssim 2$ eV.

Since the relative velocity and the overlap of the beams is not well defined in the regions where the beams are merged and demerged one must ensure that any contribution to the measured signal from these regions is negligible. In the present experiment it is easily shown that ions produced in the merging region are sufficiently deflected by fringing field of the merging magnet that they fail to reach the detector. As shown in Fig. 5, given the

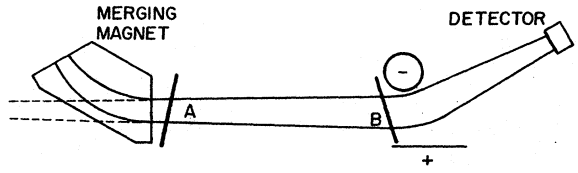

FIG. 5. Definition of interaction region length—see text.

beam energies and apparatus geometry one can establish a line in the interaction region such that ions formed upstream of the line cannot strike the detector and those created downstream can be detected. The position of this line can be determined within about ±0.5% of the total interaction region length. Downstream of line A, the ion-beam trajectory is essentially unaffected by the fringe field of the merging magnet and one may thereafter consider the ion and neutral beams to be traveling along the same axis.

Separation of the ion and neutral beams at the end of the interaction region is accomplished by an electrostatic deflecting field and, using arguments similar to those used for the merging region, one can establish a line (designated line B in Fig. 7) in the neighborhood of the deflecting field such that particles formed upstream of the line can be detected while those formed downstream cannot. In establishing line B one must account for the fact that the electrostatic potential is a function of position in the separation region.

In the present experiment, the signal is quite small, typically between 10^2 and 10^3 counts/sec, while the background count rate is large. The background arises primarily from secondary processes occurring when the parent ion and neutral beams strike metal surfaces in the interaction region and detection chamber. Typical background count rates due to the presence of the ion beam are 10^4–10^5 counts/sec while those due to the neutral beam are 10^3–10^4 counts/sec. Accurate measurement of the signal in the presence of such large background count rates presents a formidable problem. A beam modulation scheme similar to that first used by Dance *et al.*[6] provides a means of discrimination against the backgrounds. The beam modulation is accomplished by periodic application of a large voltage to the first vertical deflection plate in each beam line. As shown in Fig. 6, the two beams are modulated at the same frequency but 90° out of phase, and the scalers are gated to count four separate counting periods:

Period	Measured quantities
a	ion-beam background dark current
b	ion-beam background neutral-beam background signal dark current
c	neutral-beam background dark current
d	dark current

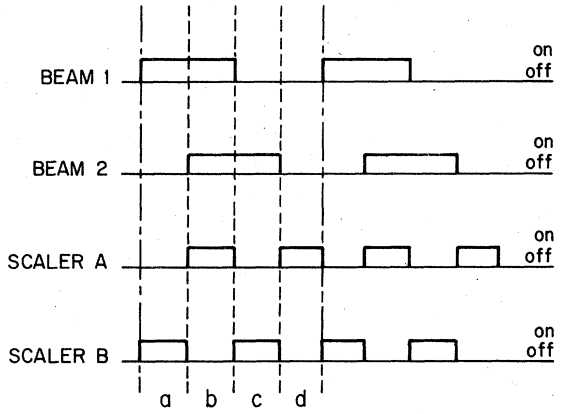

FIG. 6. Beam-modulation scheme.

The signal count rate R_s is then in principle determined by summing the count rates observed in periods b and d and subtracting the summed rates from periods a and c,

$$R_s = R_b + R_d - (R_a + R_c) . \tag{14}$$

Determination of signal with this scheme involves several tacit assumptions. The "signal" is obtained by subtraction of the sum of the count rates due to the individual presence of the ion and neutral beams from the count rate due to the combined presence of both beams. Any change in the background of one beam due to the presence of the other appears as signal. This effect has been discussed by Dolder *et al.*[7] for experiments involving colliding electron and ion beams in which the background count rate due to the ion beam is changed by the space charge of the electron beam. In merging-beam experiments these space-charge modulation problems are generally not so severe, but it is possible that the space charge of the ion beam may alter the trajectories of stripped neutrals. It is also possible (but rather unlikely at the $\sim 10^{-9}$-Torr interaction region pressure) that the space charge of slow ions formed by the passage of the neutral beam may modulate the ion-beam background. In the present experiment, a test for space-charge modulation was conducted by attempting to measure a cross section for the collision

$$\mathrm{He} + \mathrm{H}_2^+ \rightarrow \mathrm{He}^+ + H_2 , \tag{15}$$

which is highly nonresonant and is not expected to occur at low collision energies.

In attempting to measure a cross section for reaction (15) one would expect to observe effects due to space-charge cross modulation. The measured cross section for process (15) at 5-eV collision energy was 0 ± 0.23 Å^2. This result is taken to indicate that space-charge modulation effects do not contribute to the measured signal in the present experiment.

A second important assumption in the use of this modulation technique to determine the signal is that the detector and counting electronics behave linearly; that is, the registered count rate is assumed to be proportional to the rate at which ions strike the detector. However, in practice there is usually a "dead time" associated with the detector and counting electronics. Some amount of time τ (in the present experiment, ~65 nsec) is required for the detection, amplification, and registration of a single count. The counting system will not respond to a second particle striking the detector during this time. Since the probability that two or more ions will strike the detector within a 65-nsec period is proportional to the counting rate, the existence of dead time makes the counting system respond in a nonlinear fashion, with the true count rate R_T and the measured count rate R_M related by the equation

$$R_M = R_T/(1 + \tau R_T) . \tag{16}$$

Thus one must either correct the count rates measured in periods a, b, c, and d before any subtraction to determine signal is performed or one must make a dead-time-dependent correction to the measured signal count rates R_s. In the present experiment the latter course of action was chosen, and the required correction δ to R_s is given approximately by

$$\delta = 2\tau R_a R_c . \tag{17}$$

The experimental conditions are always maintained such that $\delta < 0.15 R_s$.

In the measurement of any absolute cross section it is essential that the detection efficiency for signal particles be determined. In the merging-beam experiment, one must therefore ensure that a known fraction of signal ions strike the detector and that the detector has a uniform, known efficiency over its entire area. The transport of the signal ions to the detector was examined by operating the detector under its usual conditions while sweeping a small (~0.030-in.-diam) probe beam having the same energy as the signal beam across the entrance to the detection chamber. In this way it was determined that the detection efficiency was constant for ions entering a 1.5-in.-diam circle centered on the beam axis. Absolute detection efficiency of the detector was established by directing a low-intensity beam into the detector, measuring the resulting count rate, and then deflecting the beam into a Faraday cup and measuring the resulting current. This test was per-

formed with several beams of different diameters before and after the present data were obtained, yielding the result of 0.65± 0.02 detection efficiency for the energy-analyzer–electron-multiplier combination.

A detection efficiency less than unity is a consequence of the fact that the energy analyzer transmits only about 90% of the beam incident upon it, and the electron multiplier detects only those ions that eject a secondary electron when they impinge upon the multiplier's first dynode. The fraction f of incident He^+ ions that fail to eject a secondary electron is given by

$$f = e^{-\gamma}, \tag{18}$$

where γ is the mean number of secondary electrons ejected per He^+ ion incident on the CuBe dynode. The secondary electron ejection coefficient for 1.5-keV He^+ ions incident on the activated CuBe dynode surface is expected to be between 0.8 and 3.5, depending on the past history of the surface.[8] Given that the energy-analyzer transmission is around 90%, the detection efficiency of the electron multiplier is about 75%, indicating a value for γ of 1.4, which is well within the range expected.

Taking into account the detection efficiency and the dead-time correction, the true signal S is thus given by

$$S = (R_s + \delta)/0.65. \tag{19}$$

IV. CONSISTENCY CHECKS

Several tests were carried out to verify that the apparatus would function properly under a variety of operating conditions. If the measured cross section at a particular collision energy were found to depend on the value of the overlap integral, the beam-modulation frequency, or the reactant beam energies, one would suspect the presence of a spurious effect such as modulation of the background count rate to one beam by the space charge of the other.[7]

The cross section for reaction (1) was measured at 33-eV collision energy for values of the overlap integral F spanning nearly an order of magnitude. As shown in Fig. 7, the measured cross section was independent of F. The measured cross section was also found to be independent of beam modulation frequency for frequencies between 250 and 1000 Hz.

The cross section at an energy of 30 eV in the center-of-mass was measured for four neutral beam energies between 1000 and 3000 eV, and as shown in Fig. 8, was found to be independent of neutral beam energy. This procedure also constitutes a test for the effect of excited species that may be present in the neutral beam. Since excited species would be produced only in nonresonant collisions, one would expect that a neutral beam produced by charge transfer at 3 keV would have a significantly greater population of excited species than one produced at 1 keV. The measured independence of the cross section on neutral beam energy indicates that, insofar as the present measurement is concerned, excited states do not play a significant role. One should point out that in this experiment excited species are expected not to be important since the gas used in the charge-transfer cell is helium, providing resonant charge transfer only into the ground state of He. In addition, as discussed previously, the energy analyzer discriminates against products of reactions involving excited reactants.

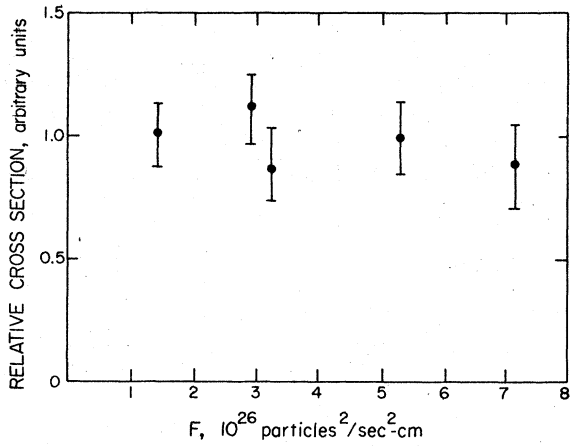

FIG. 7. Cross section for reaction (1) at 33-eV collision energy as a function of overlap integral F.

One further procedure was performed, testing both the proper function of the modulated-beam counting scheme and the validity of the dead-time correction described earlier. This procedure

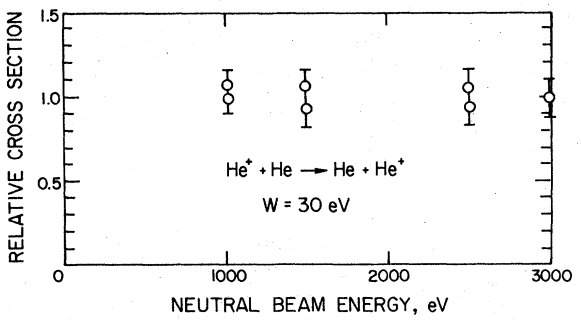

FIG. 8. Cross section for reaction (1) at 30-eV collision energy at different neutral beam energies.

involved operating the apparatus as if one were measuring signal, but without deflecting the signal into its detector. Under these conditions, large background count rates due to each of the beams are detected, but no signal is present, and thus the only contribution to the measured signal defined in Eq. (14) is the dead-time correction shown in Eq. (17). By varying the beam intensities, it was determined that the "signal" measured was given correctly by Eq. (17) over the range of count rates pertinent for the experiment.

V. KINEMATICS

In performing merging-beam experiments it is important to understand the kinematics of the collision process, since they often dictate whether or not all collision products are collected at the detector. Newton diagrams for a typical merging-beam collision are shown in Fig. 9(a), where v_1 and v_2 are the ion and neutral beam laboratory frame velocities, respectively, and u_1 and u_2 are the corresponding center-of-mass frame velocities prior to collision. The primed quantities in Fig. 9(b) refer to the same four vectors after the collision has occurred. A necessary condition for detection of a product is that the laboratory scattering angle ϕ be sufficiently small that the product will strike the detector. Clearly the maximum lab angle ϕ_{max} through which a particle can be scattered and still be detected is a function of the position in the interaction region at which the collision occurs. In the present apparatus, ϕ_{max} varies from about 1° at the beginning of the interaction region to about 2° at the end of the interaction region. For any particular set of experimental conditions, one can translate the maximum accepted lab scattering angle to a maximum accepted center-of-mass scattering angle θ_{Det}.

A further complication relating to the kinematics of the reaction arises from the fact that prior to its detection, the signal beam passes through an energy analyzer that rejects particles having substantially less energy than that of the neutral beam. Since the analyzer is of the planar-retarding-potential type, the analyzed energy ϵ_i is that corresponding to the projection of v_i on the interaction region axis, that is,

$$\epsilon_i = \tfrac{1}{2} m_i (V_{cm} + u_i' \cos\theta_i)^2 . \tag{20}$$

Clearly, the analyzed laboratory energy of the product is dependent on the center-of-mass scattering angle θ.

Assuming that the energy analyzer has infinite resolution, the maximum center-of-mass scattering angle θ_{EA} a particle can experience and still be detected is

$$\theta_{EA} = \cos^{-1}\left\{\frac{2}{v_r}\left[\left(\frac{2T_{min}}{m}\right)^{1/2} - v_{cm}\right]\right\}, \tag{21}$$

where T_{min} is the minimum energy a particle can possess and still pass through the energy analyzer. Signal particles will not be detected if their center-of-mass scattering angles exceed either θ_{Det} or θ_{EA}. Calculated values of these quantities pertinent to the present experiment appear in Table II.

One can then estimate the fraction of the signal rejected by the energy analyzer if the differential cross section for the charge transfer process is known. It is expected that for collision energies below 200 eV, product-collection efficiency decreases with decreasing collision energy because the fraction of forward-scattered product decreases significantly as one approaches low collision energies.[9] Using the data shown in Table II and a differential cross section for process (1) at 0.1-eV collision energy supplied by Bardsley,[10] we estimate that even at 0.1 eV, over 85% of the product is collected.

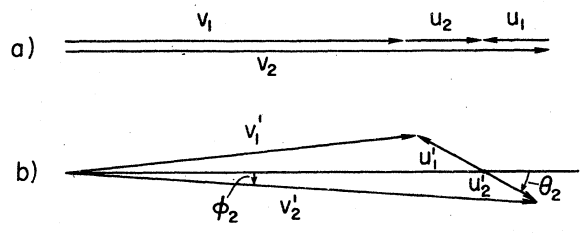

FIG. 9. Newton diagrams for merging-beam collisions.

TABLE II. Product collection limits and measured cross sections for present experiment.

Collision energy W (eV)	Measured cross section (Å²)	$^4He^+ + {}^4He$ E_{He} (eV)	E_{He^+} (eV)	θ Det	θ EA
0.1	49.7 ± 19.9 [a]	1509	1475	···[b]	94°
0.5	30.1 ± 6.2 [a]	1509	1433	···[b]	59°
1.0	27.5 ± 5.8 [a]	1509	1401	···[b]	48°
2.7	19.9 ± 4.2 [a]	1509	1335	39°	38°
6.8	21.4 ± 2.2	1509	1235	23°	29°
15	17.3 ± 3.1 [a]	3014	2442	22°	22°
33.5	15.8 ± 1.3	1509	940	10°	20°
100	13.2 ± 2.4	3014	1665	8.5°	14°
187	13.2 ± 1.6	3014	1265	6.2°	12°

[a] ^3He used in ion beam.

[b] All scattered ions remain in the solid angle subtended by the detector for these conditions.

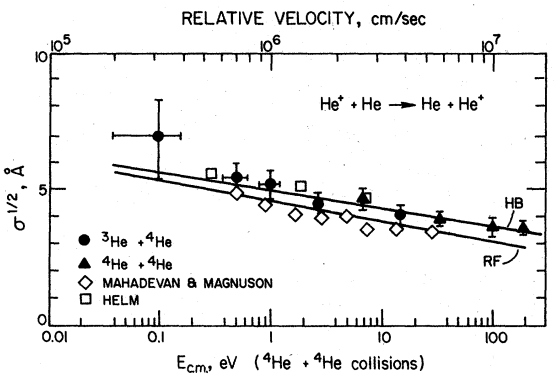

FIG. 10. Results for present study of $He^+ + He \rightarrow He + He^+$. Also shown are the experimental results of Mahadevan and Magnuson (Ref. 11), and Helm (Ref. 12). The solid curves are theoretical calculations by Hodgkinson and Briggs (Ref. 14) and Rapp and Francis (Ref. 15).

TABLE III. Net contributions of experimental parameters to uncertainties in the cross-section measurements.

	0.5 eV	7 eV	33.5 eV
Statistical uncertainty in S (1 standard deviation)	±12%	±9%	±3%
Dead-time correction	±1%	±1%	±1%
Detection efficiency	±4%	±4%	±4%
Two-dimensional overlap	±8%	±8%	±8%
Secondary electron ejection coefficient	±5%	±5%	±5%
Interaction length	±3%	±3%	±3%
Beam velocities	±0.5%	±0.5%	±0.5%
Relative velocity	±13%	±3.5%	±1.5%
Net rms uncertainty	±20.7%	±14.4%	+11.2%

VI. RESULTS

The results of the present experiment are shown in Fig. 10. As noted there, some of the points represent measurements of the charge transfer cross section

$$^3He^+ + ^4He \rightarrow ^3He + ^4He^+ . \quad (22)$$

In the energy range of this series of measurements, the differences in the charge-transfer cross sections measured using $^3He^+$ and $^4He^+$ are not expected to be significant.[9,10] Use of the lighter helium isotopes at low collision energies results in significantly lower background count rates since for a given center-of-mass collision energy, the $^3He^+$ has a lower lab energy and is deflected away from the entrance to the signal detector assembly. Also shown in Fig. 10 are the gas-cell data of Mahadevan and Magnuson[11] and the drift-tube data recently obtained by Helm.[12] There is remarkably good agreement between these data and the data of the present experiment.

A least-squares fit of the present data to the functional form $A - B \ln W$ yields the result $\sigma^{1/2} = 5.09(\pm 0.23) - 0.299(\pm 0.065) \ln W$, where σ is the cross section in Å^2 and W is the collision energy in eV. The stated uncertainties in the constants represent one standard deviation in their values.

The major sources of uncertainty in the experimental determination of the cross sections shown in Fig. 10 are summarized in Table III for three collision energies. As shown in Table III, some of the experimental uncertainties are strongly dependent on collision energy. The uncertainties in the collision energies shown by horizontal error bars in Fig. 10 are due almost entirely to uncertainty in measurement of the reactant beam velocities.

The present results also agree quite well with theory. All the calculations shown in Fig. 10 result from a semiclassical impact-parameter treatment of the collision, and the differences between the calculations are largely due to the fact that slightly different sets of He_2^+ potential curves were used in the various calculations. These semiclassical treatments agree well with conventional quantum-mechanical partial-wave treatments of the same process carried out at collision energies below 0.1 eV.[13]

ACKNOWLEDGMENTS

The authors wish to express their appreciation to John Cogan for assistance in taking data, to M. F. A. Harrison for helpful discussions and encouragement, and to the NSF, Atmospheric Sciences Section, NASA, Planetary Atmospheres Division; and the Research Corporation for financial support.

*Present address: Joint Institute for Laboratory Astrophysics, University of Colorado, Boulder, Colo. 80302.
†Present address: Lincoln Lab., P. O. Box. 73, Room E124, Lexington, Mass. 02173.

[1] B. Davis and A. H. Barnes, Phys. Rev. 34, 152 (1929).
[2] C. J. Cook and C. M. Ablow, U. S. Air Force Technical Note, AFCRC TN 59-472 (1959).

[3]S. M. Trujillo, R. H. Neynaber, and E. W. Rothe, Rev. Sci. Instrum. 37, 1665 (1966).
[4]C. F. Carlston and G. D. Magnuson, Rev. Sci. Instrum. 33, 905 (1962).
[5]D. E. Nitz, M. W. Geis, K. A. Smith, and R. D. Rundel, Rev. Sci. Instrum. 47, 306 (1976).
[6]D. F. Dance, M. F. A. Harrison, and A. C. H. Smith, Proc. R. Soc. Lond. A 290, 74 (1966).
[7]K. T. Dolder, in *Case Studies in Atomic Collision Physics*, edited by E. W. McDaniel and M. R. C. McDowell (Wiley, New York, 1969).
[8]R. Baumhäkel, Z. Phys. 199, 41 (1967).
[9]Mary Kuryian, Ph.D. thesis (York University, 1976) (unpublished).
[10]N. Bardsley (private communication).
[11]P. Mahadevan and G. D. Magnuson, Phys. Rev. 171, 103 (1968).
[12]H. Helm, in *Abstracts of Papers, Tenth International Conference on the Physics of Electronic and Atomic Collisions, Paris, 1977* (Commissariat à l'Energie Atomique, Paris, 1977).
[13]N. Lynn and B. L. Moiseiwitsch, Proc. Phys. Soc. A 70, 474 (1957).
[14]D. P. Hodgkinson and J. S. Briggs, J. Phys. B 9, 255 (1976).
[15]D. Rapp and W. E. Francis, J. Chem. Phys. 37, 2631 (1962).